L2A+

Enhanced Aeolus L2A for depolarizing targets and impact on aerosol research and NWP

-

"ASKOS ground-based datasets in support of L2A+"
Deliverable Item 02
[DI02]
(Version 2.0)

Submitted to: Christian Retscher (ESA)

	Name	Function	Date
Prepared by:	A. A. Floutsi	WP2000 – TROPOS	01/2024
	H. Baars	WP2000 – Co-I – TROPOS	01/2024
Approved by:	V. Amiridis	PI	

-

National Observatory of Athens (NOA)
Institute for Astronomy, Astrophysics, Space Applications & Remote Sensing (IAASARS)
Vas. Pavlou & I. Metaxa, 15236 Penteli, Greece
&
Leibniz Institute for Tropospheric Research (TROPOS), Leipzig, Germany
&
European Centre for Medium-Range Weather Forecasts
[ECMWF]
Reading, United Kingdom

ESA-L2A+ Deliverable Item 02 [DI02]

L2A+

Ref: *ESA AO/1-11041/22/I-NS*
ASKOS ground-based datasets in
DI02 *support of L2A+*
Page 2

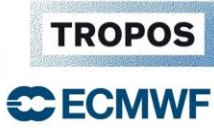[This page is intentionally left blank.]

Ref: *ESA AO/1-11041/22/I-NS*
         ASKOS ground-based datasets in
DI02   support of L2A+
Page   3

Table of Contents

Ref: *ESA AO/1-11041/22/I-NS*
L2A+   *ASKOS ground-based datasets in*
DI02   *support of L2A+*
Page   4

1. ESA-L2A+ DI02 – Overview

This document consists the Deliverable Item 02 (DI02) – Version 2 (V2) submitted to the European Space Agency (ESA) by the consortium of the project "Enhanced Aeolus L2A for depolarizing targets and impact on aerosol research and NWP" (L2A+). In accordance with WP2000, the V1 of the DI02 was initially submitted at KO + 6 months and updated at KO + 12 months.

The overall objective of WP2000 in L2A+ is to provide datasets of ground-based measurements conducted during ASKOS for the L2A+ product validation and model evaluation studies. In particular, a unique feature mask over Mindelo (D2) was created for this purpose, based on the Cloudnet and EARLINET lidar target categorization. Aerosol optical properties, wind speed (Mindelo), and radiosonde profiles obtained at Sal were also considered for the ASKOS measurement periods. Height-resolved dust properties are of high relevance for L2A+ and, therefore, POLIPHON (Mamouri and Ansmann 2014, 2016) was applied to the ground-based PollyXT lidar data to retrieve the estimation of the vertically-resolved dust fraction above Mindelo (D5). Due to the high importance of DI05 to L2A+ an earlier delivery of its V1 was succeeded at KO + 6 months, instead of the originally scheduled delivery at KO + 12. V2 of D5 is delivered as scheduled at KO + 12 months.

2. Introduction

In June 2021, within the framework of the ASKOS/JATAC campaign at Mindelo, Cape Verde (2021-2022), TROPOS deployed a ground-based, multiwavelength-Raman-polarization lidar PollyXT, a HALO wind lidar, a CIMEL sun-photometer, and an RPG microwave radiometer. All instruments were continuously measuring during all the ASKOS intensive measurement periods (September 2021, June, and September 2022).

All PollyXT lidar measurements and products have been publicly available in near-real-time via polly.tropos.de (last access: 10 January 2024).

In addition, an EarthCARE-like aerosol typing algorithm, HETEAC- Flex (Floutsi et al., 2023), was applied to the data from the ground-based lidar in Mindelo to retrieve the mixing ratio (in terms of relative volume) of four aerosol components (representing the most abundant aerosol types in nature) along with the volume concentration of mineral dust (described in detail in Section 6). Table 1 summarizes the different datasets provided within WP2000, along with their sources,

formats, availabilities and versions. In addition, tables with the complete variable list, dimensions and units for the most important WP2000 datasets is provided in the appendix. Currently, the dataset of WP2000 is hosted by NOA and the credential information can be found in DI05.

Table 1: Products delivered in the framework of L2A+ WP2000.

Products	Instrument / Source	Format	Availabiliy	Version
PollyXT Target classification	PollyXT Lidar	.nc file	September 2021, 2022 June 2022	V2
PollyXT Target classification V2	PollyXT Lidar	.nc file	September 2021, 2022 June 2022	V2
PollyXT profiles	PollyXT Lidar	.nc file	September 2021, 2022 June 2022	V2
POLIPHON	PollyXT Lidar	.nc file	September 2021, 2022 June 2022	V2
HETEAC-Flex	PollyXT Lidar	.txt file	03, 10, 17, 24 September 2021	V1
Feature mask	PollyXT Lidar	.nc file	September 2021, 2022	V1

			June 2022	
Meteorological variables	Radiosonde	.txt file	September 2021	V1

3. Data set of time series of height-resolved feature mask over Mindelo for September 2021 including aerosol optical properties

A comprehensive overview of the PollyXT lidar measurements conducted during the ASKOS intensive measurement periods is shown in Fig. 1. The attenuated backscatter coefficient at 1064 nm (Fig. 1a, 1c, 1e) in combination with the volume depolarization ratio at 532 nm (Fig. 1b, 1d, 1f) reveal that the typical aerosol conditions above Mindelo are a clean marine boundary layer (MBL; non-depolarizing spherical particles), with a dust aerosol layer (depolarizing non-spherical particles) on top of that.

For the ASKOS intensive measurement months, a total number of 1469 profiles of aerosol optical properties were derived and delivered as part of D2.
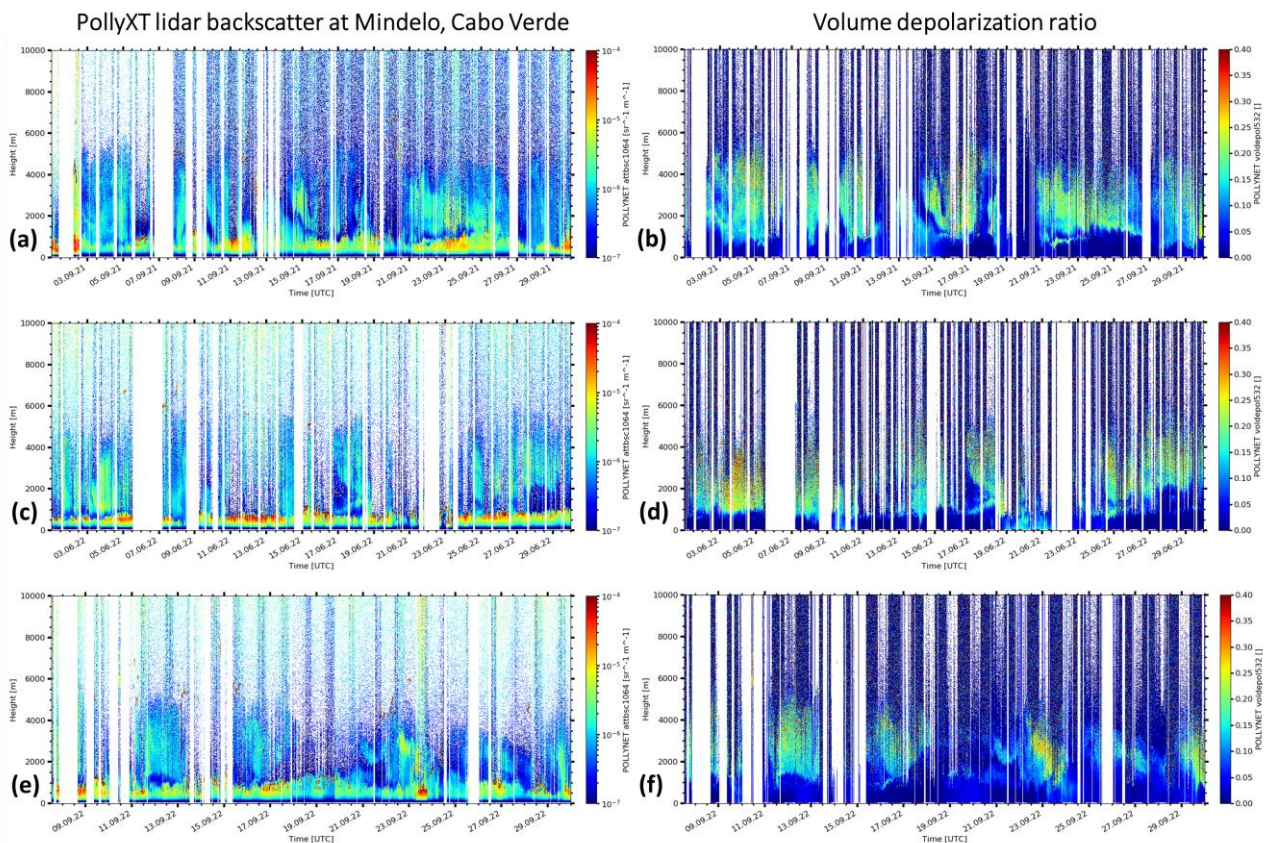

Figure 1: Overview of the lidar attenuated backscatter coefficient at 1064 nm (left column) and volume depolarization ratio at 532 nm (right column) as retrieved from the PollyXT lidar during the ASKOS operations in September 2021 (a, b), June 2022 (c, d), and September 2022 (e, f).

Based on a synergistic use of lidar and radar, a novel cloud and feature mask has been created for Mindelo. To achieve this, the EARLINET automatic target categorization based on lidar data (Baars et al., 2017) is being used in combination with the Cloudnet classification (CLU 2023) retrieved in synergistic use with ESAs cloud radar. The final product, which is the combined target classification, utilizes the aerosol classification based on the lidar data and the cloud classification from radar in a common grid. An example of this new feature mask is provided in Fig. 2. On this day (15 September

2021), we see that the MBL consists mainly of large, spherical aerosol (marine) with significant anthropogenic contributions (small aerosol) from around 06:00 to 20:00 UTC. After 20:00 UTC, liquid droplet clouds started to form. Above the MBL, between 2 and 4 km, a mineral dust aerosol layer was present. At around 12 km, a cirrus cloud was observed.

The Cloudnet target classification is one of the highest-level products, i.e., it requires several information from multiple instruments. Therefore, the creation of this target classification failed relatively often (mainly due to technical problems with the cloud radar). This was the case for several days within the ASKOS intensive measurement periods, resulting in an availability of the combined target classification mask for a total of 55 days only.
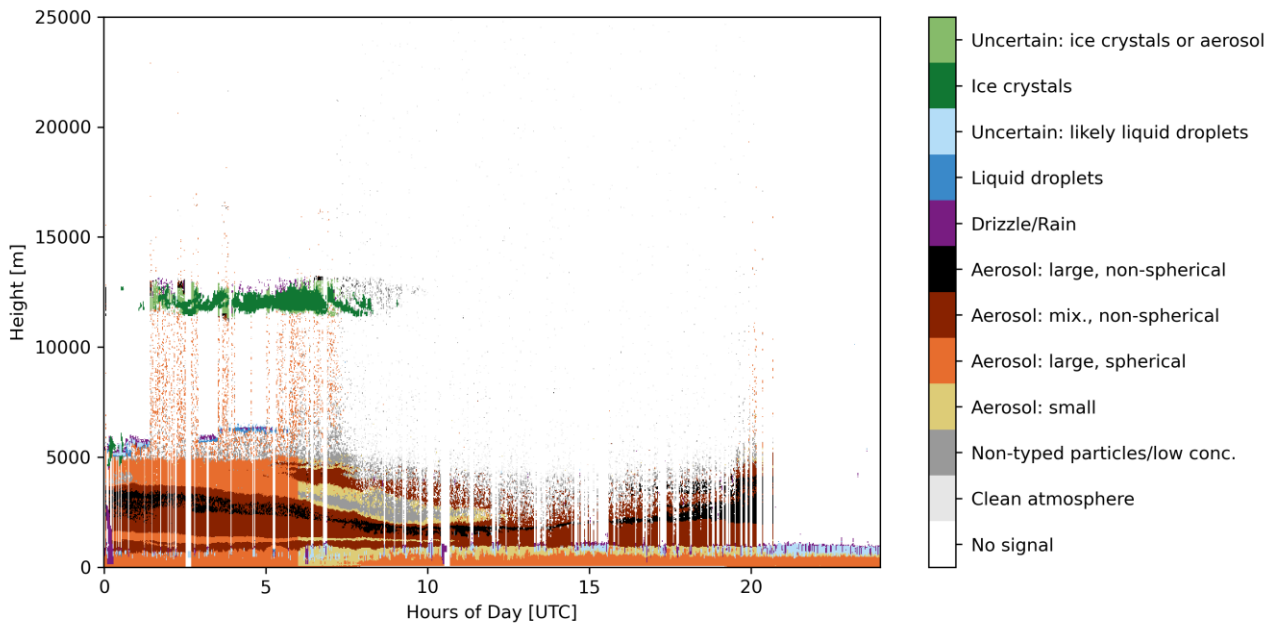

Figure 2: Combined target classification from lidar and radar synergy for 15 September 2021 at Mindelo, Cabo Verde.

4. Documentation on time series of profiles of wind speed over Mindelo and radiosonde profiles obtained at Sal

Wind speed and direction

Doppler wind lidar measurements were acquired continuously during all the ASKOS intensive measurement periods. An overview of the wind speed (a, c, e) and direction (b, d, f) for the months of September 2021 (top row), June 2022 (middle row) and September 2022 (bottom row) is shown in Fig. 3. Horizontal wind can be derived in the PBL and in the SAL in case of sufficient backscatter signal. In cases of low aerosol load (e.g., on the 20 September 2021), no winds can be derived above the PBL.

Ref: *ESA AO/1-11041/22/I-NS*
DI02 ASKOS ground-based datasets in
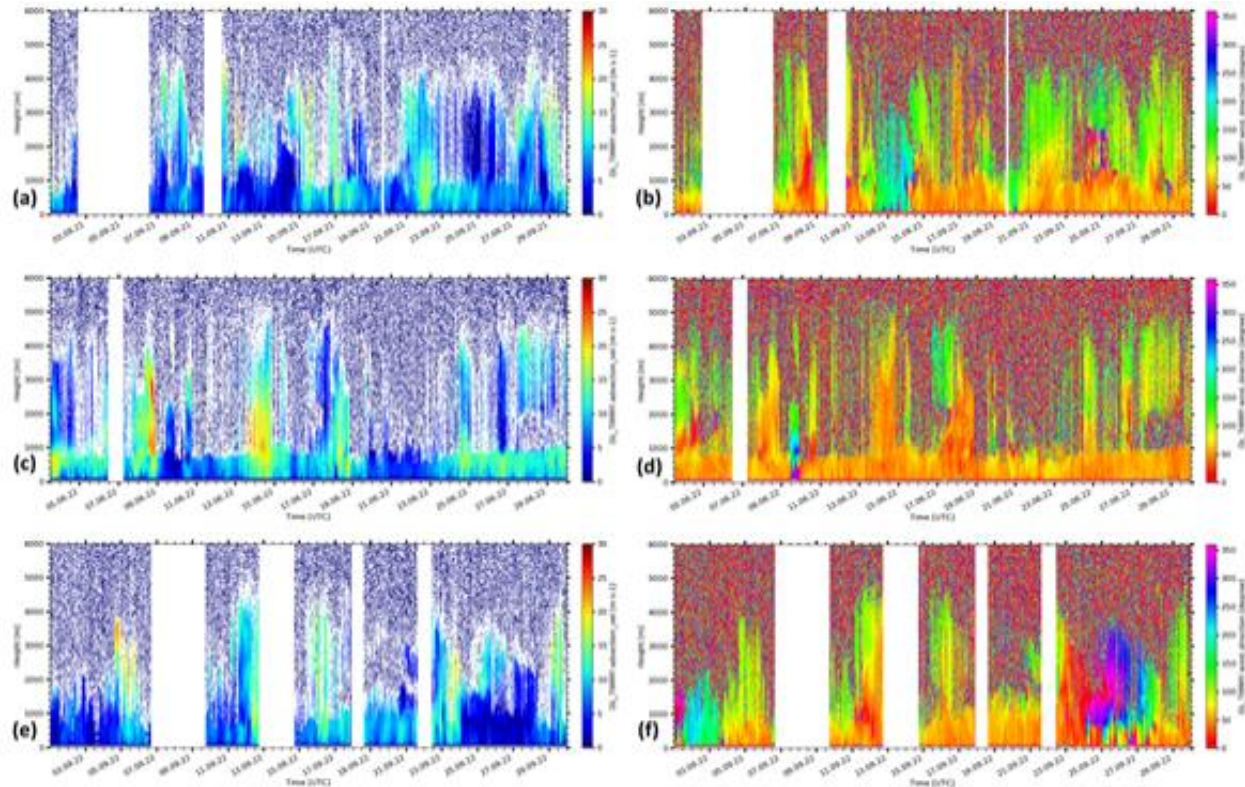support of L2A+
Page 7

L2A+

Figure 3: Overview of the Doppler wind lidar derived wind speed (left) and direction (right) during the ASKOS operations in September 2021 (a, b), June 2022 (c, d), September 2022 (e, f).

Radiosonde profiles at Sal

Radiosondes releases (Borne et al., 2023) were performed daily at Sal airport, Sal, Cabo Verde between 07 and 29 September 2021. A total number of 39 releases were performed during that time. The radiosonde schedule, which was designed to align the radiosonde releases and the Aeolus overpasses, is summarized in Table 3.

Table 2: Weekly schedule of the radiosonde releases at Sal.

Weekday	Radiosonde release time [UTC]
Monday	06:40, 10:45
Tuesday	06:50, 10:45
Wednesday	07:00, 10:45
Thursday	18:50, 10:45
Friday	19:00, 10:45
Saturday	10:45
Sunday	10:45

	L2A+	Ref:	*ESA AO/1-11041/22/I-NS*
			ASKOS ground-based datasets in
		DI02	support of L2A+
		Page	8

5. Vertically-resolved dust profiles

POLIPHON is a powerful tool that among others can be used for the separation of dust and non-dust aerosol by combining the unique capabilities of the polarisation lidar with the well-established global aerosol optical and microphysical climatologies of AERONET. The POLIPHON (Mamouri and Ansmann 2014, 2016) analysis comprises two steps. The first step is the analysis of the polarisation lidar observations based on the different polarisation properties of the different aerosol types to obtain vertically-resolved profiles of dust and non-dust backscatter coefficients, and thus the backscatter-related dust fraction. Then, by means of the appropriate dust extinction-to-backscatter ratios (lidar ratios), the dust and non-dust backscatter coefficients are converted to the respective dust and non-dust extinction coefficients. The second step of the analysis is the derivation of the vertically-resolved profile of the dust mass concentration (for both fine and coarse dust particles) from the respective extinction coefficients by utilising extinction-to-volume conversion factors that were determined from AERONET observations. Further products that can be derived with the POLIPHON method include the particle number, surface area, and volume concentration for dust and non-dust aerosol components as well as CCN and INP concentrations. For the purposes of L2A+, the two step POLIPHON analysis was performed.

The input for the first step POLIPHON, are the PollyNET profiles of backscatter, extinction and particle linear depolarization ratio at all available wavelengths. The output are vertically resolved profiles of dust and non-dust backscatter and extinction coefficients, as demonstrated in Fig. 4 for the 532-nm backscatter coefficient on 10 September 2021 between 19:00 and 19:56 UTC (within the Aeolus overpass).
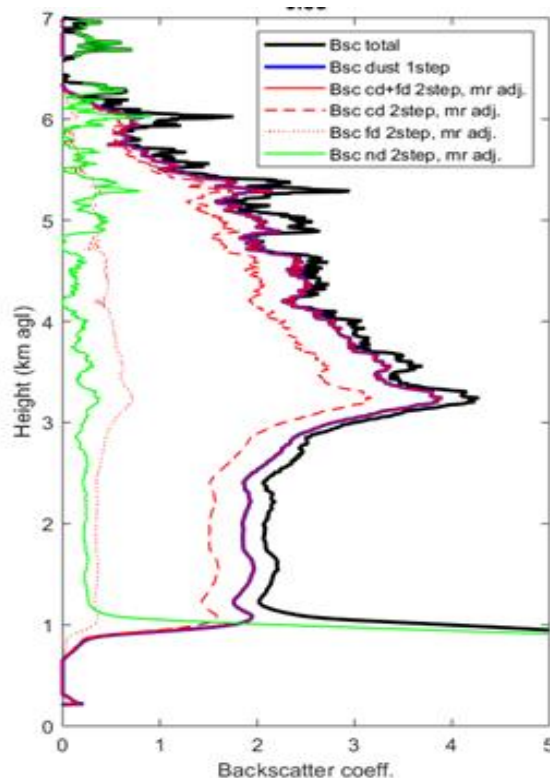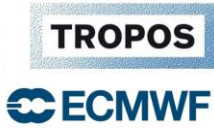

Figure 4: Dust (blue and red lines) and non-dust (green) contribution in terms of bbackscatter coefficient (PollyXT) as derived using the two-step POLIPHON methodology for Mindelo on 10 September 2021 between 19:00 and 19:56 UTC. On the second step, the dust contribution is further separated into coarse and fine mode (red dashed and dotted line, respectively).

6. HETEAC-Flex

HETEAC-Flex is an aerosol typing scheme based on the optimal estimation method applicable to both ground-based and spaceborne lidars (Floutsi et al., 2023). HETEAC-Flex is an EarthCARE-like algorithm that it is consistent with HETEAC (Hybrid End-To-End Aerosol Classification), an aerosol classification model that was developed for the EarthCARE mission (Wandinger et al., 2023).

HETEAC-Flex is being applied to retrieve the relative volume contribution of four different aerosol components, which comprise two fine (absorbing and non-absorbing) and two coarse-mode (spherical and non-spherical). The aerosol components represent the most common aerosol types observed in nature, i.e., smoke, pollution, marine and desert dust, respectively. The HETEAC-Flex results can be used to calculate additional products, including the number and volume concentration per aerosol component as well as the refractive index and effective radius of the mixture.

In Version 1 of DI02, HETEAC- Flex has been applied for the four Friday Aeolus overpasses of September 2021 (03, 10, 17 and 24). An example is shown in Fig. 5. Both, HETEAC-Flex and POLIPHON are consistent in identifying the dominance of desert dust in the aerosol layer. The non-dust POLIPHON contributions can be quantitatively attributed to three aerosol components with HETEAC- Flex.
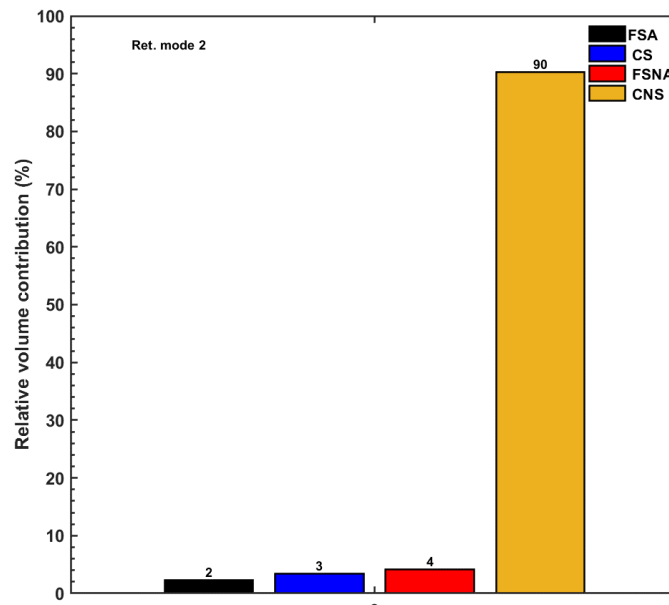
Figure 5: HETEAC-Flex results for the aerosol layer observed between 2.5 and 4 km above Mindelo on 10 September 2021 between 19:00 and 19:56 UTC. The relative volume contribution for Coarse Spherical (CS), Coarse Non-Spherical (CNS), Fine absorbing (FA) and fine none absorbing (FNA) is presented.

Ref: *ESA AO/1-11041/22/I-NS*
DI02 ASKOS ground-based datasets in
support of L2A+
Page 10

L2A+

Acronyms and Abbreviations

JATAC	Joint Aeolus Tropical Atlantic Campaign
POLIPHON	Polarisation Lidar Photometer Networking
AERONET	Aerosol Robotic Network
HETEAC	Hybrid End-To-End Aerosol Classification

List of Figures

List of Tables

ESA-L2A+ Deliverable Item 02 [DI02]

References

Baars, H., Seifert, P., Engelmann, R., and Wandinger, U.: Target categorization of aerosol and clouds by continuous multiwavelength-polarization lidar measurements, Atmos. Meas. Tech., 10, 3175–3201, https://doi.org/10.5194/amt-10-3175-2017, 2017.
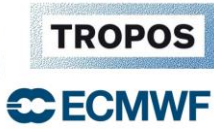
Borne, M., Knippertz, P., Weissmann, M., Witschas, B., Flamant, C., Rios-Berrios, R., and Veals, P.: Validation of Aeolus L2B products over the tropical Atlantic using radiosondes, EGUsphere [preprint], https://doi.org/10.5194/egusphere-2023-742, 2023.

CLU (2023): Cloud profiling product: Classification; 2021-09-09 to 2021-09-30; from Mindelo. Generated by the cloud profiling unit of the ACTRIS Data Centre, https://hdl.handle.net/21.12132/2.bbd79a556daa477d, 2023.

Floutsi, A. A., Baars, H., and Wandinger, U.: HETEAC-Flex: An optimal estimation method for aerosol typing based on lidar-derived intensive optical properties, EGUsphere [preprint], https://doi.org/10.5194/egusphere-2023-1880, 2023.

Mamouri, R. E. and Ansmann, A.: Fine and coarse dust separation with polarization lidar, Atmos. Meas. Tech., 7, 3717–3735, https://doi.org/10.5194/amt-7-3717-2014, 2014.

Mamouri, R.-E. and Ansmann, A.: Potential of polarization lidar to provide profiles of CCN- and INP-relevant aerosol parameters, Atmos. Chem. Phys., 16, 5905–5931, https://doi.org/10.5194/acp-16-5905-2016, 2016.

Wandinger, U., Floutsi, A. A., Baars, H., Haarig, M., Ansmann, A., Hünerbein, A., Docter, N., Donovan, D., van Zadelhoff, G.-J., Mason, S., and Cole, J.: HETEAC – the Hybrid End-To-End Aerosol Classification model for EarthCARE, Atmos. Meas. Tech., 16, 2485–2510, https://doi.org/10.5194/amt-16-2485-2023, 2023.

Appendix

The unique height-resolved feature mask utilizes multiwavelength-Raman-polarization lidar, cloud radar and microwave radiometer data and allows for high-performance cloud and feature detection (Combined Cloudnet + EARLINET lidar target categorization).

The filenames follow the structure: "YYYYMMDD_regridded_data_for_mindelo.nc"

Group	Subgroup	Variable	Units	Dimensions	Description
FEATURE MASK	-	cloudnet_LWP	g/m²	1D	Liquid water path
		cloudnet_radar_gas_attenuation	dB	2D	Two-way radar attenuation due to atmospheric gases
		cloudnet_radar_liquid_attenuation	dB	2D	Two-way radar attenuation due to liquid water
		cloudnet_radar_v	m/s	2D	Doppler velocity
		cloudnet_radar_width	m/s	2D	Spectral width
		cloudnet_radar_Z	dBZ	2D	Radar reflectivity factor

ESA-L2A+ Deliverable Item 02 [DI02]

	Ref:	*ESA AO/1-11041/22/I-NS*
L2A+		ASKOS ground-based datasets in
	DI02	support of L2A+
	Page	12

		cloudnet_radar_Z_error	dB	2D	Error in radar reflectivity factor
		cloudnet_target_classification	1	2D	Target classification
		combined_target_classification	1	2D	Novel feature mask
		height	m	1D	Height above mean sea level
		model_pressure	Pa	2D	Pressure
		model_temperature	K	2D	Temperature
		polly_ang_532_1064	1	2D	Quasi backscatter-related Ångström exponent at 532-1064 nm
		polly_att_bsc_1064	sr^{-1} m^{-1}	2D	Attenuated backscatter at 1064 nm
		polly_att_bsc_532	sr^{-1} m^{-1}	2D	Attenuated backscatter at 532 nm
		polly_bsc_1064	sr^{-1} m^{-1}	2D	Quasi aerosol backscatter coefficients at 1064 nm
		polly_bsc_1064_quality_flag	1	2D	QC information
		polly_bsc_532	sr^{-1} m^{-1}	2D	Quasi aerosol backscatter coefficients at 532 nm
		polly_bsc_532_quality_flag	1	2D	QC information
		polly_pardepol_532	1	2D	quasi particle depolarization ratio at 532 nm
		polly_target_classification	1	2D	EARLINET lidar classification
		polly_voldepol_532	1	2D	Volume depolarization ratio at 532 nm
		polly_voldepol_532_quality_flag	1	2D	QC information
		time	UTC	1D	Hours of day

The dataset also includes vertically-resolved aerosol optical properties derived from the PollyXT ground-based, multiwavelength, Raman, polarization lidar measurements.

The filenames follow the structure:
"YYYY_MM_DD_weekday_CPV_HH_MM_SS_HHMM_HHMM_profiles.nc"

Group	*Subgroup*	*Variable*	*Units*	*Dimensions*	*Description*
PollyXT PROFILES	-	aerBsc_aeronet_1064	sr^{-1} m^{-1}	1D	Aerosol backscatter coefficient at 1064 nm retrieved with constrained-AOD method
		aerBsc_aeronet_355	sr^{-1} m^{-1}	1D	Aerosol backscatter coefficient at 355 nm retrieved with
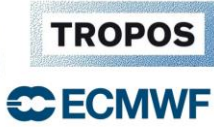
						constrained-AOD method
		aerBsc_aeronet_532	sr⁻¹ m⁻¹	1D		Aerosol backscatter coefficient at 532 nm retrieved with constrained-AOD method
		aerBsc_klett_1064	sr⁻¹ m⁻¹	1D		Aerosol backscatter coefficient at 1064 nm retrieved with Klett method
		aerBsc_klett_355	sr⁻¹ m⁻¹	1D		Aerosol backscatter coefficient at 355 nm retrieved with Klett method
		aerBsc_klett_532	sr⁻¹ m⁻¹	1D		Aerosol backscatter coefficient at 532 nm retrieved with Klett method
		aerBsc_raman_1064	sr⁻¹ m⁻¹	1D		Aerosol backscatter coefficient at 1064 nm retrieved with Raman method
		aerBsc_raman_355	sr⁻¹ m⁻¹	1D		Aerosol backscatter coefficient at 355 nm retrieved with Raman method
		aerBsc_raman_532	sr⁻¹ m⁻¹	1D		Aerosol backscatter coefficient at 532 nm retrieved with Raman method
		aerBsc_RR_1064	sr⁻¹ m⁻¹	1D		Aerosol backscatter coefficient at 1064 nm retrieved with rotation Raman method
		aerBsc_RR_355	sr⁻¹ m⁻¹	1D		Aerosol backscatter coefficient at 355 nm retrieved with rotation Raman method
		aerBsc_RR_532	sr⁻¹ m⁻¹	1D		Aerosol backscatter coefficient at 532 nm retrieved with rotation Raman method
		aerExt_raman_1064	m⁻¹	1D		Aerosol extinction coefficient at 1064 nm retrieved with Raman method
		aerExt_raman_355	m⁻¹	1D		Aerosol extinction coefficient at 355 nm retrieved with Raman method
		aerExt_raman_532	m⁻¹	1D		Aerosol extinction coefficient at 532 nm retrieved with Raman method

ESA-L2A+ Deliverable Item 02 [DI02]

aerExt_RR_1064	m⁻¹	1D	Aerosol extinction coefficient at 1064 nm retrieved with rotation Raman method
aerExt_RR_355	m⁻¹	1D	Aerosol extinction coefficient at 355 nm retrieved with rotation Raman method
aerExt_RR_532	m⁻¹	1D	Aerosol extinction coefficient at 532 nm retrieved with rotation Raman method
aerLR_raman_1064	sr	1D	Aerosol lidar ratio at 1064 nm retrieved with Raman method
aerLR_raman_355	sr	1D	Aerosol lidar ratio at 355 nm retrieved with Raman method
aerLR_raman_532	sr	1D	Aerosol lidar ratio at 532 nm retrieved with Raman method
aerLR_RR_1064	sr	1D	Aerosol lidar ratio at 1064 nm retrieved with rotation Raman method
aerLR_RR_355	sr	1D	Aerosol lidar ratio at 355 nm retrieved with rotation Raman method
aerLR_RR_532	sr	1D	Aerosol lidar ratio at 532 nm retrieved with rotation Raman method
altitude	m	-	Height of lidar above mean sea level
end_time	seconds since 1970-01-01 00:00:00 UTC	-	Time UTC of the end of the current measurement
height	m	1D	Height above ground
latitude	degrees north	-	Latitude of the site
longitude	degrees east	-	Longitude of the site
LR_aeronet_1064	sr	-	Aerosol lidar ratio at 1064 nm retrieved with constrained-AOD method
LR_aeronet_355	sr	-	Aerosol lidar ratio at 355 nm retrieved

					with constrained-AOD method
		LR_aeronet_532	sr	-	Aerosol lidar ratio at 532 nm retrieved with constrained-AOD method
		parDepol_klett_1064	1	1D	Particle linear depolarization ratio at 1064 nm with Klett backscatter
		parDepol_klett_355	1	1D	Particle linear depolarization ratio at 355 nm with Klett backscatter
		parDepol_klett_532	1	1D	Particle linear depolarization ratio at 532 nm with Klett backscatter
		parDepol_raman_1064	1	1D	Particle linear depolarization ratio at 1064 nm with Raman backscatter
		parDepol_raman_355	1	1D	Particle linear depolarization ratio at 355 nm with Raman backscatter
		parDepol_raman_532	1	1D	Particle linear depolarization ratio at 532 nm with Raman backscatter
		pressure	hPa	1D	Air pressure
		reference_height_1064	m	1D	Reference height for 1064 nm
		reference_height_355	m	1D	Reference height for 355 nm
		reference_height_532	m	1D	Reference height for 532 nm
		RH	%	1D	Relative humidity
		shots	1	-	Accumulated laser shots
		start_time	seconds since 1970-01-01 00:00:00 UTC	-	Time UTC of the start of the current measurement
		temperature	degree Celsius	1D	Air temperature
		uncertainty_aerBsc_aeronet_1064	$sr^{-1}\,m^{-1}$	1D	Uncertainty of aerosol backscatter coefficient at 1064 nm
		uncertainty_aerBsc_aeronet_355	$sr^{-1}\,m^{-1}$	1D	Uncertainty of aerosol backscatter coefficient at 355 nm

L2A+

		uncertainty_aerBsc_aeronet_532	sr⁻¹ m⁻¹	1D	Uncertainty of aerosol backscatter coefficient at 532 nm
		uncertainty_aerBsc_klett_1064	sr⁻¹ m⁻¹	1D	Uncertainty of aerosol backscatter coefficient at 1064 nm
		uncertainty_aerBsc_klett_355	sr⁻¹ m⁻¹	1D	Uncertainty of aerosol backscatter coefficient at 355 nm
		uncertainty_aerBsc_klett_532	sr⁻¹ m⁻¹	1D	Uncertainty of aerosol backscatter coefficient at 532 nm
		uncertainty_aerBsc_raman_1064	sr⁻¹ m⁻¹	1D	Uncertainty of aerosol backscatter coefficient at 1064 nm
		uncertainty_aerBsc_raman_355	sr⁻¹ m⁻¹	1D	Uncertainty of aerosol backscatter coefficient at 355 nm
		uncertainty_aerBsc_raman_532	sr⁻¹ m⁻¹	1D	Uncertainty of aerosol backscatter coefficient at 532 nm
		uncertainty_aerBsc_RR_1064	sr⁻¹ m⁻¹	1D	Uncertainty of aerosol backscatter coefficient at 1064 nm
		uncertainty_aerBsc_RR_355	sr⁻¹ m⁻¹	1D	Uncertainty of aerosol backscatter coefficient at 355 nm
		uncertainty_aerBsc_RR_532	sr⁻¹ m⁻¹	1D	Uncertainty of aerosol backscatter coefficient at 532 nm
		uncertainty_aerExt_raman_1064	m⁻¹	1D	Uncertainty of aerosol extinction coefficient at 1064 nm
		uncertainty_aerExt_raman_355	m⁻¹	1D	Uncertainty of aerosol extinction coefficient at 355 nm
		uncertainty_aerExt_raman_532	m⁻¹	1D	Uncertainty of aerosol extinction coefficient at 532 nm
		uncertainty_aerExt_RR_1064	m⁻¹	1D	Uncertainty of aerosol extinction coefficient at 1064 nm
		uncertainty_aerExt_RR_355	m⁻¹	1D	Uncertainty of aerosol extinction coefficient at 355 nm
		uncertainty_aerExt_RR_532	m⁻¹	1D	Uncertainty of aerosol extinction coefficient at 532 nm
		uncertainty_aerLR_raman_1064	m⁻¹	1D	Uncertainty of aerosol lidar ratio at 1064 nm

		uncertainty_aerLR_raman_355	sr	1D	Uncertainty of aerosol lidar ratio at 355 nm	
		uncertainty_aerLR_raman_532	sr	1D	Uncertainty of aerosol lidar ratio at 532 nm	
		uncertainty_aerLR_RR_1064	sr	1D	Uncertainty of aerosol lidar ratio at 1064 nm	
		uncertainty_aerLR_RR_355	sr	1D	Uncertainty of aerosol lidar ratio at 355 nm	
		uncertainty_aerLR_RR_532	sr	1D	Uncertainty of aerosol lidar ratio at 532 nm	
		uncertainty_parDepol_klett_1064	1	1D	Uncertainty of particle linear depolarization ratio at 1064 nm with Klett backscatter	
		uncertainty_parDepol_klett_355	1	1D	Uncertainty of particle linear depolarization ratio at 355 nm with Klett backscatter	
		uncertainty_parDepol_klett_532	1	1D	Uncertainty of particle linear depolarization ratio at 532 nm with Klett backscatter	
		uncertainty_parDepol_raman_1064	1	1D	Uncertainty of particle linear depolarization ratio at 1064 nm with Raman backscatter	
		uncertainty_parDepol_raman_355	1	1D	Uncertainty of particle linear depolarization ratio at 355 nm with Raman backscatter	
		uncertainty_parDepol_raman_532	1	1D	Uncertainty of particle linear depolarization ratio at 532 nm with Raman backscatter	
		uncertainty_volDepol_klett_1064	1	1D	Uncertainty of volume depolarization ratio at 1064 nm	
		uncertainty_volDepol_klett_355	1	1D	Uncertainty of volume depolarization ratio at 355 nm	
		uncertainty_volDepol_klett_532	1	1D	Uncertainty of volume depolarization ratio at 532 nm	

Ref: *ESA AO/1-11041/22/I-NS*
ASKOS ground-based datasets in
DI02 support of L2A+
Page 18

L2A+

		uncertainty_volDepol_raman_1064	1	1D	Uncertainty of volume depolarization ratio at 1064 nm
		uncertainty_volDepol_raman_355	1	1D	Uncertainty of volume depolarization ratio at 355 nm
		uncertainty_volDepol_raman_532	1	1D	Uncertainty of volume depolarization ratio at 532 nm
		uncertainty_WVMR	g/km	1D	Absolute water vapor mixing ratio uncertainty
		volDepol_klett_1064	1	1D	Volume linear depolarization ratio at 1064 nm with the same smoothing as Klett method
		volDepol_klett_355	1	1D	Volume linear depolarization ratio at 355 nm with the same smoothing as Klett method
		volDepol_klett_532	1	1D	Volume linear depolarization ratio at 532 nm with the same smoothing as Klett method
		volDepol_raman_1064	1	1D	Volume linear depolarization ratio at 1064 nm with the same smoothing as Raman method
		volDepol_raman_355	1	1D	Volume linear depolarization ratio at 355 nm with the same smoothing as Raman method
		volDepol_raman_532	1	1D	Volume linear depolarization ratio at 532 nm with the same smoothing as Raman method
		WVMR	g/kg	1D	Water vapor mixing ratio
		WVMR_no_QC	g/kg	1D	Water vapor mixing ratio without quality control
		WVMR_rel_err	1	1D	Relative error of the water vapor mixing ratio
		zenith_angle	degree	-	Zenith angle

The 1-step POLIPHON methodology was applied to the PollyXT ground-based lidar data to derive the height-resolved dust-only optical properties.

The filename follows the structure:
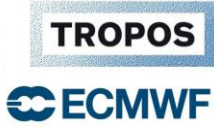"YYYY_MM_DD_weekday_CPV_HH_MM_SS_HHMM_HHMM _POLIPHON_1.nc"

Group	Subgroup	Variable	Units	Dimensions	Description
DUST-ONLY (POLIPHON-1) PROFILES	-	aerBsc1064_klett_d1	$sr^{-1}\,m^{-1}$	1D	One-step dust particle backscatter coefficient at 1064 nm retrieved with Klett method
		aerBsc1064_klett_nd1	$sr^{-1}\,m^{-1}$	1D	One-step non-dust particle backscatter coefficient at 1064 nm retrieved with Klett method
		aerBsc1064_raman_d1	$sr^{-1}\,m^{-1}$	1D	One-step dust particle backscatter coefficient at 1064 nm retrieved with Raman method
		aerBsc1064_raman_nd1	$sr^{-1}\,m^{-1}$	1D	One-step non-dust particle backscatter coefficient at 1064 nm retrieved with Raman method
		aerBsc355_klett_d1	$sr^{-1}\,m^{-1}$	1D	One-step dust particle backscatter coefficient at 355 nm retrieved with Klett method
		aerBsc355_klett_nd1	$sr^{-1}\,m^{-1}$	1D	One-step non-dust particle backscatter coefficient at 355 nm retrieved

L2A+

					with Klett method
	aerBsc355_raman_d1	sr⁻¹ m⁻¹	1D		One-step dust particle backscatter coefficient at 355 nm retrieved with Raman method
	aerBsc355_raman_nd1	sr⁻¹ m⁻¹	1D		One-step non-dust particle backscatter coefficient at 355 nm retrieved with Raman method
	aerBsc532_klett_d1	sr⁻¹ m⁻¹	1D		One-step dust particle backscatter coefficient at 532 nm retrieved with Klett method
	aerBsc532_klett_nd1	sr⁻¹ m⁻¹	1D		One-step non-dust particle backscatter coefficient at 532 nm retrieved with Klett method
	aerBsc532_raman_d1	sr⁻¹ m⁻¹	1D		One-step dust particle backscatter coefficient at 532 nm retrieved with Raman method
	aerBsc532_raman_nd1	sr⁻¹ m⁻¹	1D		One-step non-dust particle backscatter coefficient at 532 nm retrieved with Raman method
	aerBsc_klett_1064	sr⁻¹ m⁻¹	1D		Aerosol backscatter coefficient at 1064 nm retrieved

					with Klett method
		aerBsc_klett_355	sr⁻¹ m⁻¹	1D	Aerosol backscatter coefficient at 355 nm retrieved with Klett method
		aerBsc_klett_532	sr⁻¹ m⁻¹	1D	Aerosol backscatter coefficient at 532 nm retrieved with Klett method
		aerBsc_raman_1064	sr⁻¹ m⁻¹	1D	Aerosol backscatter coefficient at 1064 nm retrieved with Raman method
		aerBsc_raman_355	sr⁻¹ m⁻¹	1D	Aerosol backscatter coefficient at 355 nm retrieved with Raman method
		aerBsc_raman_532	sr⁻¹ m⁻¹	1D	Aerosol backscatter coefficient at 532 nm retrieved with Raman method
		altitude	m	-	Height of lidar above mean sea level
		end_time	seconds since 1970-01-01 00:00:00 UTC	-	Time UTC of the end of the current measurement
		height	m	1D	Height above ground
		latitude	degrees north	-	Latitude of the site
		longitude	degrees east	-	Longitude of the site
		start_time	seconds since 1970-01-01	-	Time UTC of the start of the current measurement

The units in the table: $sr^{-1}\,m^{-1}$

Ref: *ESA AO/1-11041/22/I-NS*
ASKOS ground-based datasets in
DI02   support of L2A+
Page   22

L2A+

			00:00:00 UTC		
		time	seconds since 1970-01-01 00:00:00 UTC	1D	Time
		uncertainty_aerBsc1064__n d1	sr⁻¹ m⁻¹	1D	Uncertainty of one-step non-dust particle backscatter coefficient at 1064 nm retrieved with Klett method
		uncertainty_aerBsc1064_klett_d1	sr⁻¹ m⁻¹	1D	Uncertainty of one-step dust particle backscatter coefficient at 1064 nm retrieved with Klett method
		uncertainty_aerBsc1064_raman_d1	sr⁻¹ m⁻¹	1D	Uncertainty of one-step dust particle backscatter coefficient at 1064 nm retrieved with Raman method
		uncertainty_aerBsc1064_raman_nd1	sr⁻¹ m⁻¹	1D	Uncertainty of one-step non-dust particle backscatter coefficient at 1064 nm retrieved with Raman method
		uncertainty_aerBsc355_klett_d1	sr⁻¹ m⁻¹	1D	Uncertainty of one-step dust particle backscatter coefficient at 355 nm retrieved with Klett method
		uncertainty_aerBsc355_klett_nd1	sr⁻¹ m⁻¹	1D	Uncertainty of one-step non-dust particle

Ref: *ESA AO/1-11041/22/I-NS*
L2A+   ASKOS ground-based datasets in
DI02   support of L2A+
Page   23

						backscatter coefficient at 355 nm retrieved with Klett method
			uncertainty_aerBsc355_raman_d1	sr⁻¹ m⁻¹	1D	Uncertainty of one-step dust particle backscatter coefficient at 355 nm retrieved with Raman method
			uncertainty_aerBsc355_raman_nd1	sr⁻¹ m⁻¹	1D	Uncertainty of one-step non-dust particle backscatter coefficient at 355 nm retrieved with Raman method
			uncertainty_aerBsc532_klett_d1	sr⁻¹ m⁻¹	1D	Uncertainty of one-step dust particle backscatter coefficient at 532 nm retrieved with Klett method
			uncertainty_aerBsc532_klett_nd1	sr⁻¹ m⁻¹	1D	Uncertainty of one-step non-dust particle backscatter coefficient at 532 nm retrieved with Klett method
			uncertainty_aerBsc532_raman_d1	sr⁻¹ m⁻¹	1D	Uncertainty of one-step dust particle backscatter coefficient at 532 nm retrieved with Raman method
			uncertainty_aerBsc532_raman_nd1	sr⁻¹ m⁻¹	1D	Uncertainty of one-step non-dust particle backscatter

L2A+

					coefficient at 532 nm retrieved with Raman method
		uncertainty_aerBsc_klett_1064	sr^{-1} m^{-1}	1D	Uncertainty of aerosol backscatter coefficient at 1064 nm
		uncertainty_aerBsc_klett_355	sr^{-1} m^{-1}	1D	Uncertainty of aerosol backscatter coefficient at 355 nm
		uncertainty_aerBsc_klett_532	sr^{-1} m^{-1}	1D	Uncertainty of aerosol backscatter coefficient at 532 nm
		uncertainty_aerBsc_raman_1064	sr^{-1} m^{-1}	1D	Uncertainty of aerosol backscatter coefficient at 1064 nm
		uncertainty_aerBsc_raman_355	sr^{-1} m^{-1}	1D	Uncertainty of aerosol backscatter coefficient at 355 nm
		uncertainty_aerBsc_raman_532	sr^{-1} m^{-1}	1D	Uncertainty of aerosol backscatter coefficient at 532 nm

Ref: *ESA AO/1-11041/22/I-NS*
DI02 ASKOS ground-based datasets in
support of L2A+
Page 25

L2A+

[End of ESA-L2A+ DI02 - "ASKOS Datasets"]